

In situ measurement of growth stress in alumina scale

E. D. Specht^{a)} and P. F. Tortorelli

Metals and Ceramics Division, Oak Ridge National Laboratory, Oak Ridge, Tennessee 37831-6118

P. Zschack

University of Illinois at Urbana-Champaign, Argonne, Illinois 60439

(Received 3 September 2003; accepted 12 December 2003)

Stress in the early stages of growth has been measured in α -Al₂O₃ (alumina) scales formed on FeCrAl- and NiAl-based alloys during heating in air at 1000 °C to 1200 °C. Scale thickness ranges from 0.5 to 5 μ m, times from 5 to 720 min. Stress was measured using the multiple-tilt method. In order to measure the thinnest scales at the earliest times, focused, monochromatic synchrotron radiation was used for high intensity, and a fixed, small angle of incidence was used along with an appropriate wavelength to maximize scattering from the film relative to the background from the substrate. Depending on the composition, transient tensile stresses of up to 1.2 GPa were observed, with maximum stress at times ranging from >10 h at 1000 °C to <10 min at 1200 °C. Thermal stresses induced by an abrupt temperature change were found to relax much more quickly, suggesting that the kinetics observed during isothermal growth reflect a dynamic competition between stress generation and stress relaxation. These results challenge commonly accepted models of growth stress in scales that predict that a compressive stress will be generated as the metal converts to a larger-volume oxide in a constrained location such as an interface. The observed tensile stress may be due to another mechanism altogether (e.g., grain coalescence), or to the conversion of a transitional Al₂O₃ to the equilibrium α -Al₂O₃ phase. For one composition, transitional Al₂O₃ is observed during the period of tensile stress. © 2004 International Centre for Diffraction Data. [DOI: 10.1154/1.1649318]

INTRODUCTION

Certain metals can be used at elevated temperatures in oxidizing environments due to the formation of a protective scale, an oxide film that limits further oxidation. The useful life of these materials will be limited if the scale cracks and spalls, so it is important to understand and control the stress in the scale that can drive this failure. When the metal is heated or cooled, thermally induced stress arises from the difference in thermal expansion coefficients between metal and oxide; thermal stress and its effects on oxidation are relatively well understood (Evans, 1989; Schütze, 1997; Evans, 1994). However, stress development when the metal is held at a constant temperature while the oxide grows is not well understood. Even the sign of the resulting growth stress is debated. Still less is known about the magnitude and the effects on failure (Evans and Cannon, 1989; Stott and Atkinson, 1994; Cannon and Hou, 1998; Nix and Clemens, 1999; Pilling and Bedworth, 1923).

One source of the poor understanding of growth stress is the variety of possible mechanisms. Epitaxial stress occurs when a film strains to match the lattice constant of the substrate. If the film has the larger (smaller) lattice parameter, it will grow under compression (tension). A volume change will induce stress if the material is constrained as it changes volume. Since metal typically expands as it oxidizes, oxide that grows under a constraint such as growth in the grain boundary will be under compression. Finally, surface tension can induce stress. Since a film has a lower energy when its surface is smooth, a film with a rough surface will deform to decrease this roughness, putting the film under tension.

A further impediment to the understanding of growth stress is the difficulty of measurement. Growth stress is most

often measured by monitoring the bending of the substrate (Floro *et al.*, 2001), which is not a practical technique for metal substrates, which deform plastically at elevated temperatures. Further, one side must be protected from oxidation, and film thickness must be known to measure stress. Quantitative, *in situ* data from scales on metal substrates has come from the X-ray diffraction measurement of strain (Sarioglu *et al.*, 1997, 2000; Schumann *et al.*, 2000). Using previous techniques, such a measurement takes an hour or more, so the early stages of growth cannot be monitored. We have used intense synchrotron radiation to make stress measurements in \sim 5 min. Pioneering measurements are presented of growth stress in its early stages.

The oxide microstructure of these samples, studied with transmission electron microscopy, is published elsewhere, along with a preliminary account of the growth stress results (Tortorelli *et al.*, 2003).

EXPERIMENTAL

The alloy compositions were based on the FeCrAl and NiAl systems (Table I). The Kanthal AF alloy was a commercial rolled ribbon while the other two FeCrAl-based alloys were made at Oak Ridge National Laboratory by arc melting, casting, hot extrusion, and rolling to sheet. The FeCrAl-based specimens (approximately 1 \times 5–7 \times 100 mm) were cut from the ribbon or sheet, annealed, and mechanically polished to a 0.3 μ m diamond-paste surface finish. The two NiAl alloys were cast into rectangular plates from which specimens (approximately 1 \times 10 \times 100 mm) were electro-discharge machined, and then electropolished.

High X-ray intensity is provided by focused, monochromatic undulator radiation at beamline 33-ID-D of the Advanced Photon Source, with a beam size at the specimen of \sim 0.25 \times 0.2 mm² and intensity of \sim 10¹³ photons/s. Stress was measured by comparing plane spacings for one Bragg

^{a)} Electronic mail: specht@ornl.gov

TABLE I. Compositions of alloys used in this study (concentrations in at. % except for S).

	Fe	Ni	Cr	Al	Other	S (ppma)
FeCrAlY	70.1		20.1	9.8	0.035 Y	<4
Kanthal AF	67		21	11	0.5 Si, 0.08 Zr	
Ni-43Al		57		43		
Ni-43Al-Hf		57		43	0.06 Hf	

reflection measured at multiple tilts. Several modifications have been made to the standard multiple tilt method (Noyan and Cohen, 1987) in order to analyze thin films at high temperatures. As sample temperature increases, atomic thermal vibrations lead to a decrease in Bragg peak intensity and an increase in diffuse background scattering. The problem of a low signal to background ratio is compounded in the early stages of growth, where the film is thin, giving a low signal, while the substrate is thick, giving a large background. Three measures are taken to increase the signal to background ratio. First, measurements are taken at lower Bragg angles, where Bragg peaks are more intense and the diffuse background less so. The (116) reflection of α -Al₂O₃ was used except where noted. Several samples were repeated using the (214) reflection, with no significant differences in results. These lower-angle reflections are less sensitive to strain, so data must be collected with higher angular resolution to get the same sensitivity to stress. Second, the angle of incidence is kept fixed at 80° from the surface normal to reduce the penetration of the beam into the substrate and limit the diffuse scattering from it. Third, an X-ray energy of 9 keV is used; this is above the K absorption edges of Cr, Fe, and Ni, an energy that further reduces the penetration of the beam into the substrate and thus diffuse scattering. An undesirable side effect of this choice of energy is high fluorescence from Cr, Fe, and Ni. This fluorescence is filtered out by a graphite (002) diffracted-beam monochromator.

The use of lower Bragg angles increases sensitivity to sample displacements: stress measurements are most often taken close to a Bragg angle of 180°, where sample displacement causes no error at all. As noted above, higher angular resolution is needed for lower Bragg angles, so it is critical to eliminate sample displacement errors. This is done using a parallel beam geometry. The incident beam is parallel to within 0.01°, a characteristic of undulator radiation, and the diffracted beam angle is defined by soller slits, parallel plates of Mo with a length of 100 mm, and a spacing of 0.18 mm. Peaks are typically 0.15° FWHM; the peak center can be determined with uncertainty of 0.015°, corresponding to an uncertainty of 3×10^{-4} in strain and 100 MPa in stress.

Conventional X-ray furnaces were not suitable for these measurements. These typically surround the sample with thermal insulators and reflectors to create a region of controlled temperature with minimal power consumption. The result is that the sample takes too long to come to thermal equilibrium at an elevated temperature, and the narrow apertures provided for X-ray access do not allow multiple tilt measurements at a constant angle of incidence. Both these problems are addressed using a novel furnace with neither shielding nor insulation. The sample is cast or rolled in rectangular form, roughly 0.5 mm × 10 mm × 100 mm, clamped between water-cooled electrodes, and resistively heated by ac current. One electrode is mounted on a spring-loaded slide

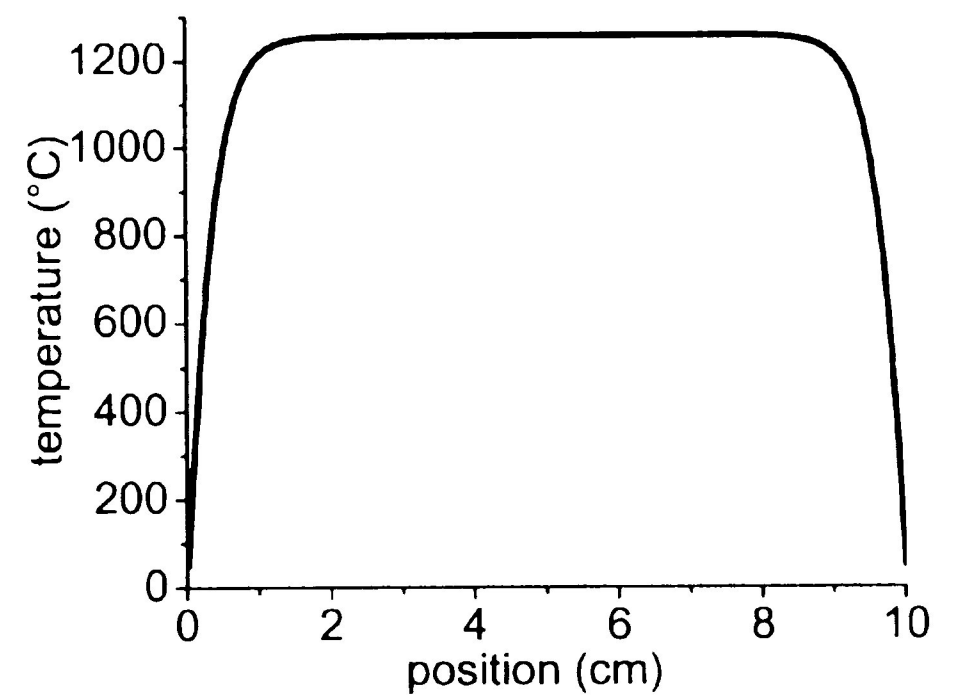


Figure 1. Calculated temperature profile for Kanthal A.

to take up thermal expansion of the sample. Temperature was controlled using a Pt/Pt10%Rh (type S) thermocouple spot-welded to the sample about 5 mm away from the point where X-rays were incident on the sample, but on the opposite surface. This avoids diffraction from the thermocouple while minimizing the temperature difference between the thermocouple and the sample.

As discussed above, sample displacement does not affect the accuracy of stress measurement. Still, it is essential that the X-rays hit the sample face. A fluorescent crystal was mounted behind the sample and a video camera is used to observe the shadow that the sample casts on this crystal when illuminated with X-rays. Al foil was used to shield the crystal from the visible light emitted by the hot sample. The sample was lowered until the incident beam just passes the sample, then raised so the beam hits the center of the sample face. This procedure was repeated each time the sample temperature is changed.

The sample reaches thermal equilibrium rapidly at temperatures above ~ 500 °C, where heat loss is primarily radiative. Starting from room temperature, the temperature can be stabilized at 800 °C to 1200 °C within 30 s. The temperature profile is calculated by numerically solving the heat equation,

$$C\rho \frac{dT}{dt} = \rho_E \left(\frac{I}{tw} \right)^2 - \frac{2\varepsilon\sigma T^4}{t} + \kappa \frac{d^2T}{dx^2}, \quad (1)$$

where C is heat capacity, ρ density, T temperature, ρ_E electrical resistivity, I electrical current, t thickness, w width, ε emissivity, σ the Stefan Boltzmann constant, κ thermal conductivity, and x position. We consider only radiation from the sample faces, neglecting the edges. Taking, for example, Kanthal A, $C = 4600$ J/kg K, $\rho = 7.1 \times 10^3$ kg/m³, $\rho_E = 1.45 \times 10^{-6}$ Ω m, $t = 0.5$ mm, $w = 10$ cm, $\varepsilon = 0.7$, $\sigma = 5.7 \times 10^{-8}$ W/m² K⁴, and $\kappa = 11$ W/m K (Kanthal Handbook). Taking $I = 118$ A and iterating Eq. (1) until T converges gives the profile in Figure 1.

The calculated temperature profile is very uniform: T varies by <1 K over the central 6 cm. The temperature falls to room temperature over a region whose length is proportional to $\sqrt{\kappa t/T^3}$; the sample must be long and thin to have a wide region of uniform temperature. Temperature uniformity is, in fact, limited by the uniformity of sample thickness. A 10% variation in sample thickness will lead to a 2.5% variation in temperature.

Each stress measurement comprised five 2θ scans over a range of tilts from 30° to 66°. In the frame of the sample, the X-ray beam was incident at a fixed angle while the detector

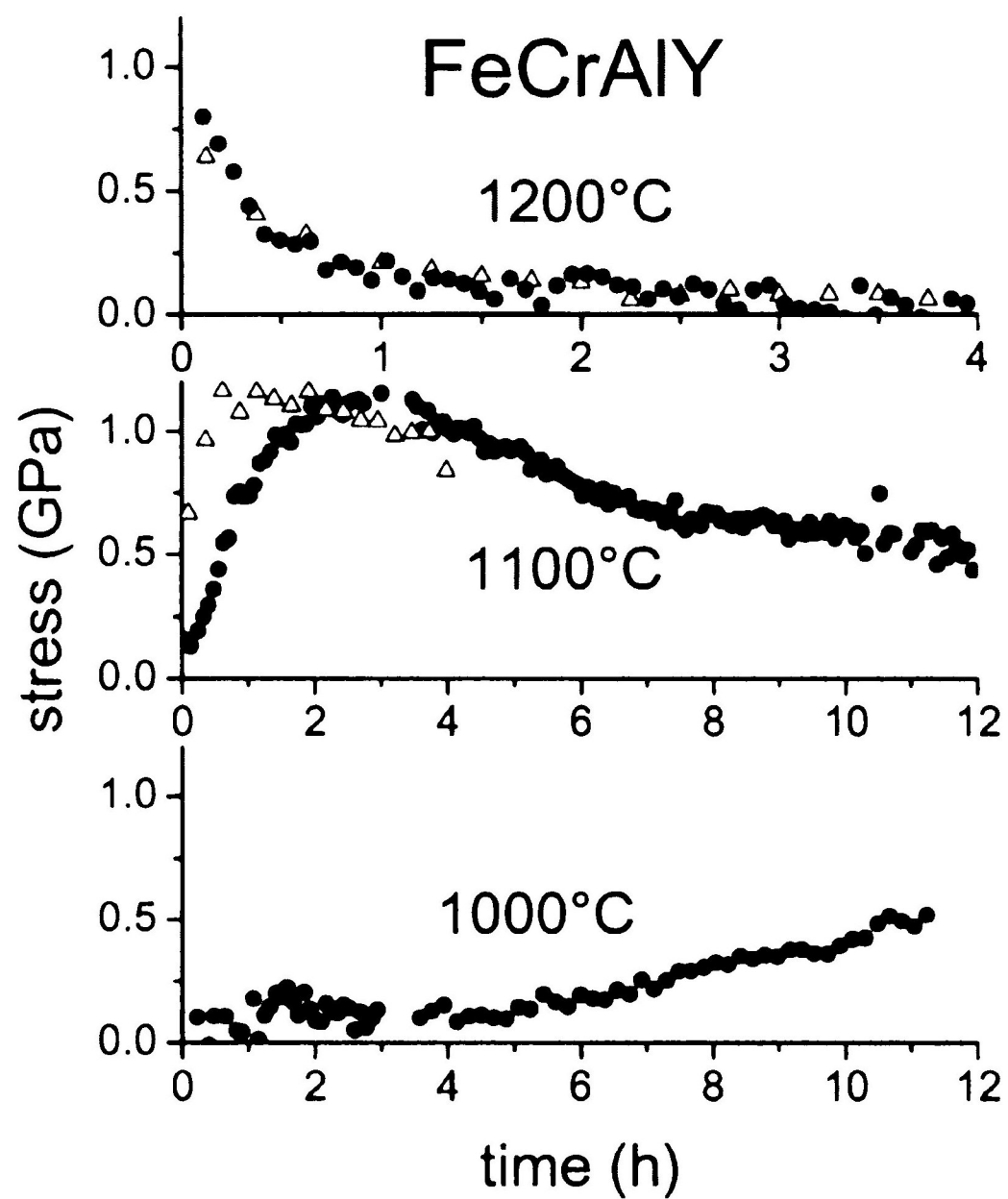


Figure 2. Growth stress for FeCrAlY. Different symbols denote repeated runs with similar samples.

rotated in an arc at a fixed Bragg angle. In the lab frame, this was accomplished by setting the four-circle Euler angles (Busing and Levy, 1966) to $\phi=0$ and ω and χ chosen to solve $\cos(\alpha)=\sin(\chi)\sin(\theta_B + \omega)$ (fixed glancing angle) and $\cos(\psi)=\sin(\chi)\cos(\omega)$ (proper tilt), where θ_B is the Bragg angle, α the angle of incidence, and ψ the desired tilt. A linear variation of plane spacing with $\sin^2 \psi$ was observed, to within instrumental uncertainty. Each stress measurement took from 5 to 15 min.

Al_2O_3 Bragg angles were determined by least squares fitting of observed peaks with Lorentzian squared lineshapes. The Al_2O_3 reflection from the FeCrAlY sample all have a broader, low-angle shoulder, most likely from a second phase of Al_2O_3 that contains another metal substituting for Al, dilating the lattice. These were fit as a second peak, and results from the more intense, sharper, higher-angle peak were used. Strain was inferred from the slope of the 2θ vs $\sin^2 \Psi$ plot using linear regression. This method does not require *a priori* knowledge of the lattice parameter, so uncertainty regarding the temperature or composition does not affect the accuracy of the stress measurement. This multiple-tilt method of stress analysis is described in Noyan and Cohen, 1987. $\alpha\text{-Al}_2\text{O}_3$ is sufficiently isotropic that the Voigt and Reuss methods (Noyan and Cohen, 1987) give equivalent results for inferring stress from strain, using the temperature-dependent elastic constants (Goto *et al.*, 1989).

RESULTS

Growth stress for FeCrAlY is shown in Figure 2. At 1000 °C, scattering was initially weak and diffuse, and stress could be measured only after about 15 min. At 1200 °C, measurement time was the limiting factor; the first 5 min stress measurement revealed sharp peaks. All three temperatures are consistent with the same qualitative behavior: stress rises from zero to a maximum of 1.2 GPa (tensile), then falls back to zero. The time scale varies dramatically, so only the rising stress is observed at 1000 °C, only the falling stress at

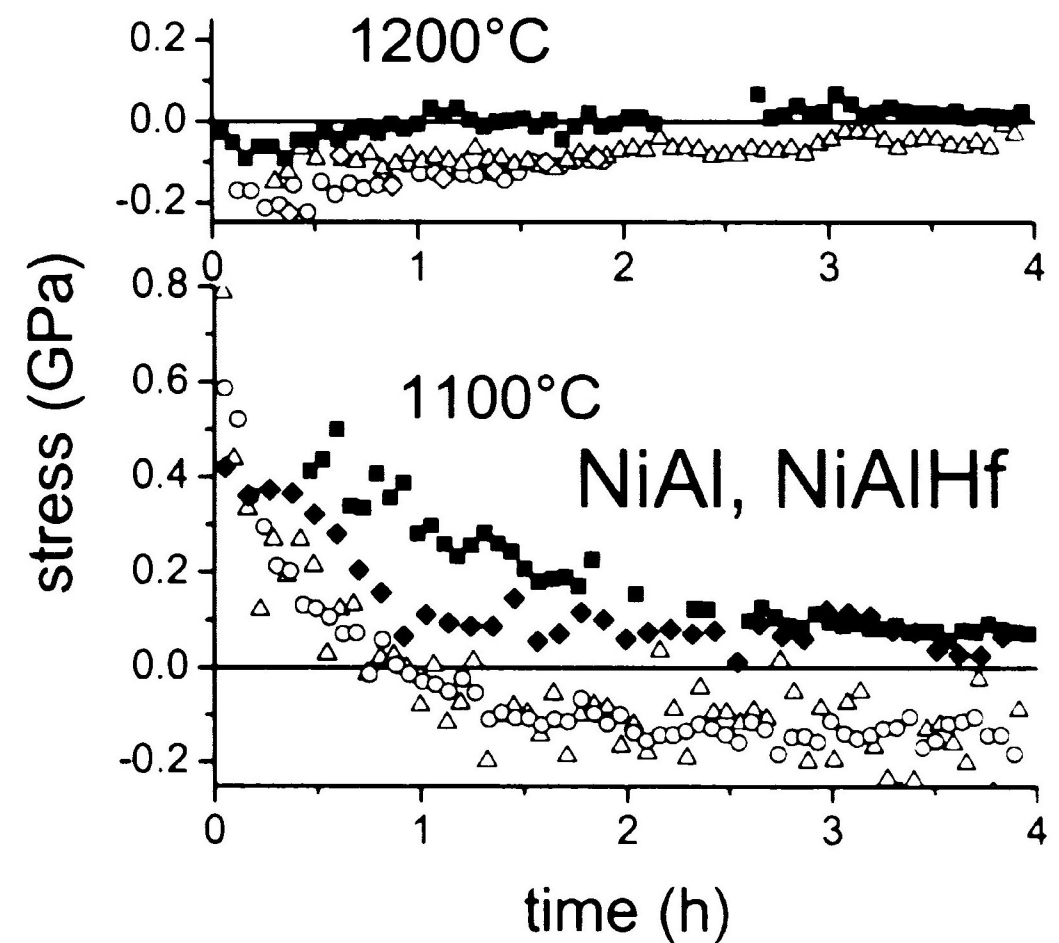


Figure 3. Growth stress for NiAl and NiAlHf. Open symbols: NiAl. Closed symbols: NiAlHf.

1200 °C, while both are seen at 1100 °C. Different symbols on the plots denote repeated measurements on different samples. Reproducibility is good, except for variability in the time scale. Because the time scale changes greatly with temperature; this variability indicates a difference of $\sim 10^\circ\text{C}$ in temperature, that can be attributed to nonuniform sample thickness, as discussed above.

Both NiAl alloys (Figure 3) exhibit behavior similar to FeCrAlY, although if there is a period of increasing stress it is too fast to measure. The stress is already falling off during the first measurements at 1100 °C and 1200 °C and measurements at 1000 °C (not shown) show the growth of spinel phases rather than $\alpha\text{-Al}_2\text{O}_3$. Stress in NiAlHf falls to zero as for FeCrAlY, while the initial tensile stress reverses to a compressive stress of ~ -0.2 GPa for NiAl.

No significant growth stress was seen in Kanthal AF (not shown), although $\alpha\text{-Al}_2\text{O}_3$ formed at 1000 °C, 1100 °C, and 1200 °C.

Stress relaxation was studied by observing the decay of a thermal stress applied by abruptly changing the sample temperature. Figure 4 shows both the change in lattice parameter, a measure of temperature, and the stress as the temperature of FeCrAlY is changed in 100 °C increments following the growth of $\alpha\text{-Al}_2\text{O}_3$ for 2 h at 1200 °C. The tensile stress is initially falling off as in Figure 3. Abrupt decreases (increases) in temperature add a compressive (tensile) stress component. While the relaxation behavior is complex and we will not attempt to explain it here, it is clear that relaxation of the thermal stress is much faster than the falloff of growth stress.

Compressive stress relaxes over 5 to 30 min at 800 °C to 1100 °C, and in <5 min at 1200 °C. Tensile stress relaxes in <5 min at all temperatures.

Al_2O_3 can form as metastable "transitional" Al_2O_3 , as well as stable $\alpha\text{-Al}_2\text{O}_3$ (Grabke, 1999). The transitional phases are modifications of the cubic spinel structure (Levin and Brandon, 1998). Stress measurements were repeated using the $\text{Al}_2\text{O}_3(113)$ reflection, taking a wide enough scan to include scattering from the (400) reflection of the spinel structure. Measurements were taken at 1000 °C and 1100 °C, where transitional Al_2O_3 has been reported to form (Grabke, 1999). Only $\alpha\text{-Al}_2\text{O}_3$ is observed for FeCrAlY. A peak at the (400) spinel Bragg angle is observed for Kanthal and

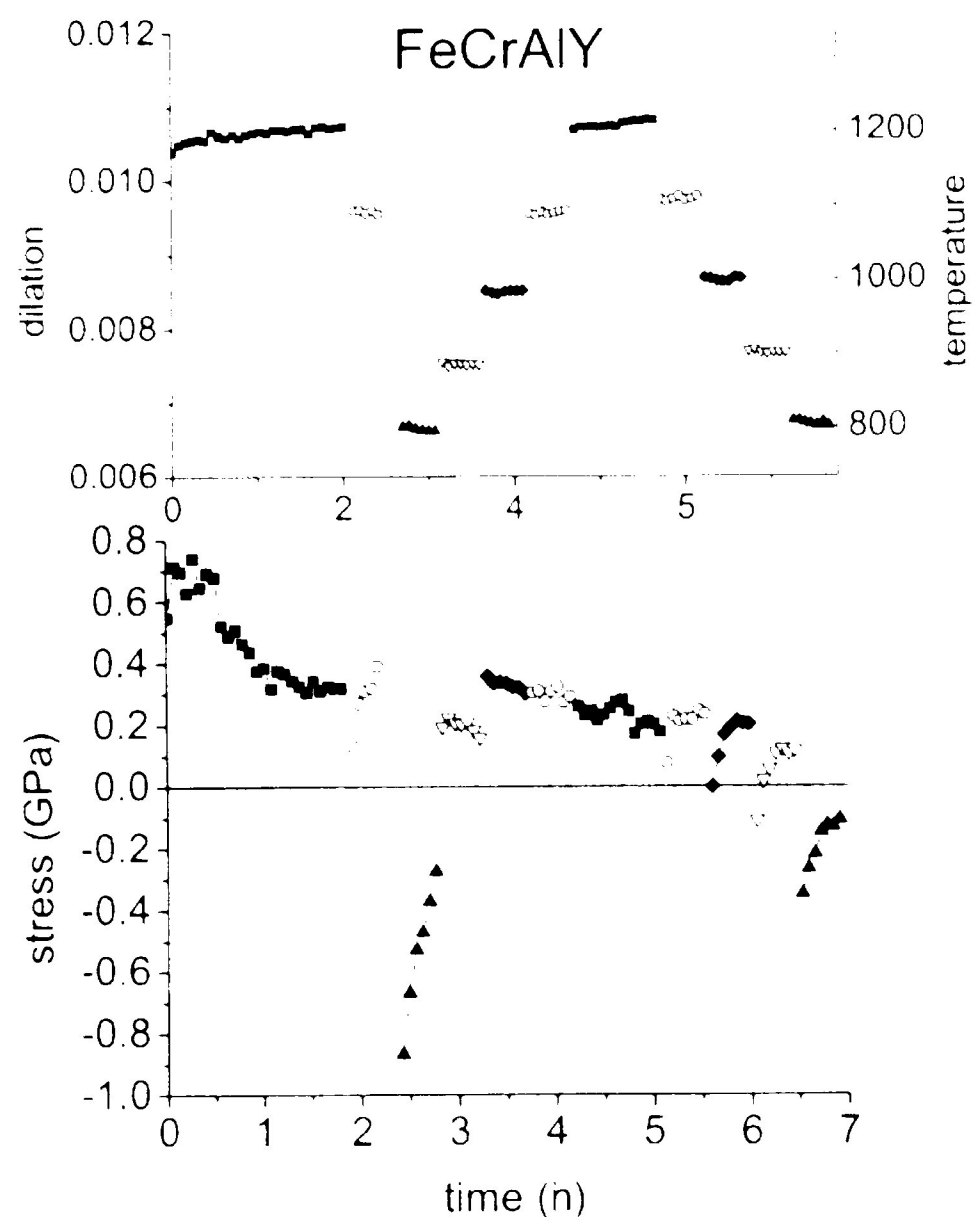


Figure 4. Relaxation of thermal stress. Upper panel: temperature profile; lower panel: stress.

NiAlHf, but it grows along with α -Al₂O₃ rather than transforming to α -Al₂O₃, so it is more likely to be a stable spinel such as NiCr₂O₄, Fe(Cr,Al)₂O₄, or NiAl₂O₄.

Only for NiAl does the signature of transitional Al₂O₃ appear. A split peak occurs at the (400) Bragg angle, along with the α -Al₂O₃ peaks (Figure 5), growing for ~15 min then converting to α -Al₂O₃ (Fig. 6). Tensile stress is observed in α -Al₂O₃ while transitional Al₂O₃ appears. Stress could not be measured for transitional Al₂O₃ because the peaks are broad, weak, and overlapping.

DISCUSSION

Intense synchrotron radiation allows measurement of growth stress in the early stages of growth. Using a laboratory X-ray source, Schumann *et al.* could measure a growth stress for α -Al₂O₃ on NiAl at 1100 °C only after four hours of growth (Schumann *et al.*, 2000). The result, zero stress, is consistent with this work, but misses the large, transient tensile stress that can be observed using synchrotron radiation (Figure 3). The Sarioglu *et al.* results for FeCrAlY are in poor agreement, finding *compressive* stresses of 0.5 to 1.4 GPa after several hours at 1000 °C and 1100 °C while in this work we report a ~0.5 GPa *tensile* stress (Figure 2). This

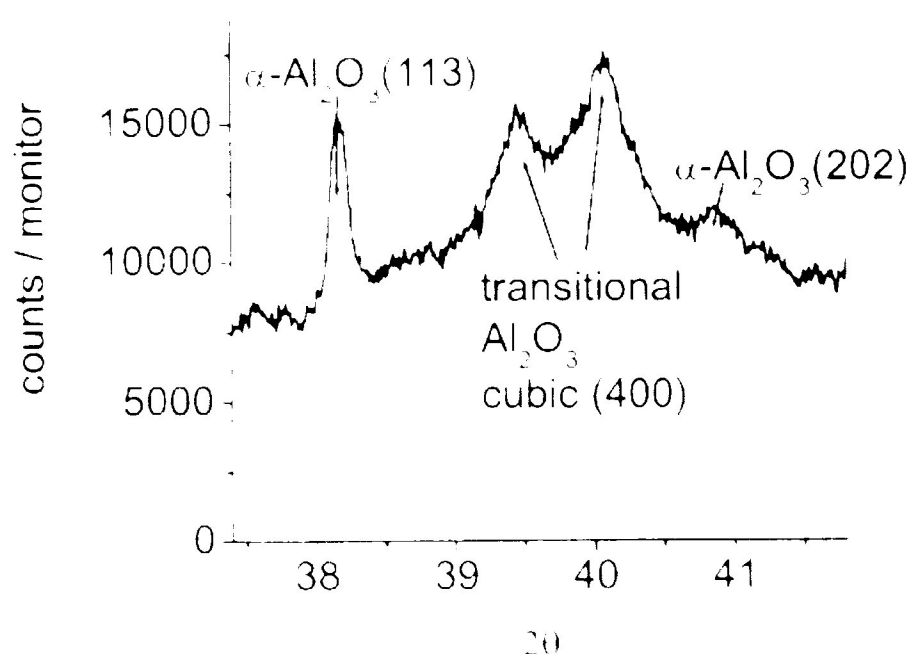


Figure 5. NiAl, 1100 °C, 6 min

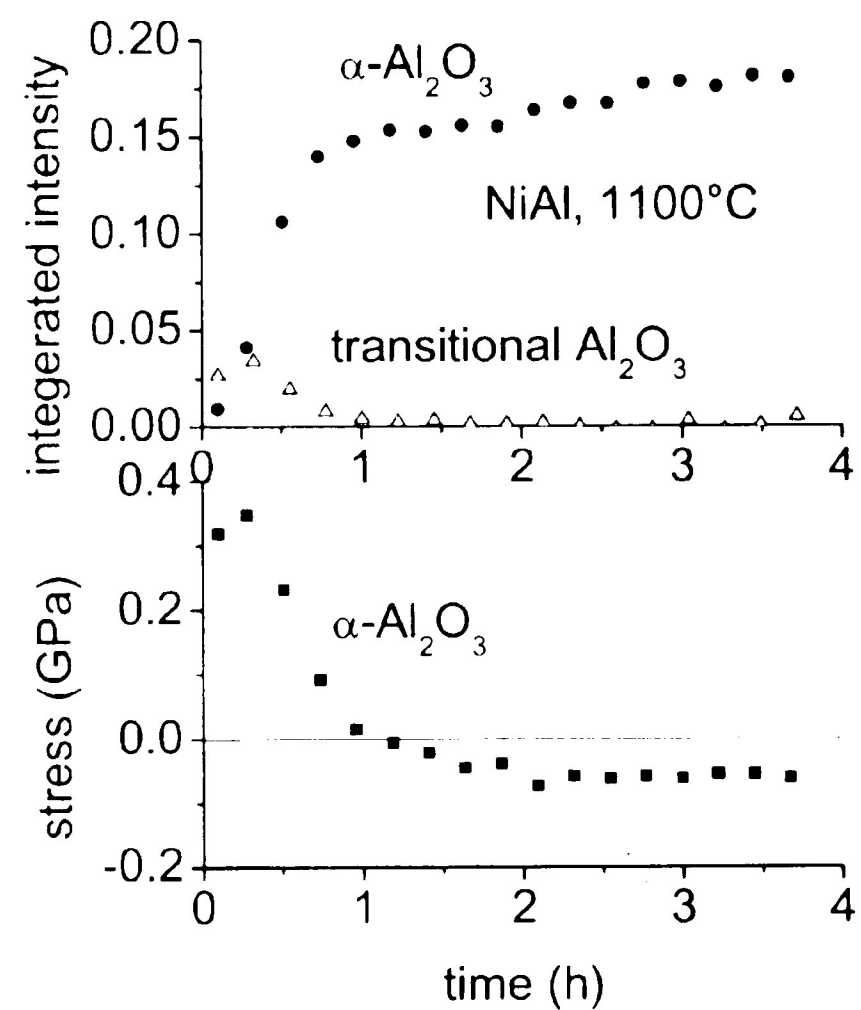


Figure 6. (upper) Integrated area of α -Al₂O₃(113) and transitional Al₂O₃(400) Bragg reflections; (lower) growth stress in α -Al₂O₃.

discrepancy is far outside any uncertainty in measurement, so we attribute it to a difference in samples. Scale growth on FeCrAlY is known to be sensitive to S, among other elements (Messoudi *et al.*, 2000); the S content of Sarioglu's samples is not reported. Veal *et al.* are using synchrotron radiation to study growth stress in scale grown on single crystals of NiAl; preliminary results show an initial tensile stress of ~0.6 GPa, falling to zero in ~3 h (Veal).

The only large growth stresses that we have observed are tensile. Reviews of growth stress in oxide scales suggest that "the major cause of stress is associated with a change in volume as the metal is converted into oxide" (Stott and Atkinson, 1994; Pilling and Bedworth, 1923; Huntz, 1988). For the reaction $\text{Fe}_{70}\text{Cr}_{20}\text{Al}_{10} \rightarrow 0.99(\text{Fe}_{70.7}\text{Cr}_{20.2}\text{Al}_{9.1}) + 0.5\text{Al}_2\text{O}_3$, the Pilling–Bedford ratio (PBR, a measure of this expansion) is 1.17 (relatively small because the alloy contracts as it becomes depleted in Al), while for the oxidation of Ni₅₀Al₅₀ the PBR is 1.77 (there is no significant volume change in this alloy due to compositional changes). Because both are greater than 1, the volume change would cause a compressive stress. We must look to less conventional mechanisms to explain the observed growth stress.

By measuring the relaxation of applied thermal stresses, it is seen that stress relaxes in 5 min or less at temperatures of 1000 °C or above (Figure 4). Assuming that growth stresses relax by the same mechanism as thermal stresses, this implies that the relatively slow relaxation of growth stress is determined, not by relaxation mechanisms, but by a dynamic equilibrium between the generation and relaxation of stress. Since stress is most likely generated at the growth front where the new oxide scale is formed, a natural explanation for the decreasing growth stress lies in the increasing thickness of the oxide. Even if the level of stress generated by growth is constant at the growth front, this is averaged over the whole thickness of the film, reducing the average stress that is measured by diffraction. A qualitatively similar time dependence for the average stress in alumina scale on FeCrAlY has been calculated by assuming that the new scale is formed with a constant growth stress while the scale stress relaxes by substrate creep (Bull, 1998).

A possible cause of tensile stress is the volume change when transitional Al₂O₃ converts to α -Al₂O₃: volume de-

creases, giving a PBR of ~ 0.85 . The temporal coincidence of transitional Al_2O_3 and growth stress in NiAl (Figure 6) supports this mechanism. However, a tensile stress is unexpected when the total reaction of metal to oxide has $\text{PBR} > 1$. The reaction of metal to transitional Al_2O_3 will occur at the metal–oxide interface, where the metal may accommodate stress by deforming plastically or be less constrained, while the final conversion to $\alpha\text{-Al}_2\text{O}_3$ occurs at an oxide–oxide interface, where stress cannot be so readily relaxed. A more serious objection is that while transitional Al_2O_3 can account for tensile stress in NiAl, it is not observed in NiAlHf or FeCrAlY, so another mechanism would be needed to account for growth stress in this alloy. An explanation that accounted for all results would be more compelling.

While a transient tensile growth stress is the opposite of that predicted by Pilling and Bedford (1923), it is similar to the behavior observed for thin films grown by physical vapor deposition (Floro *et al.*, 2001). For a variety of metals grown on amorphous and polycrystalline Si and Ge, growth stress starts near zero, reaches a maximum tensile stress, falls to zero, then reverses to a smaller compressive stress. The tensile growth stress is attributed to crystallite coalescence (Nix and Clemens, 1999). As growing crystallites contact each other at their bases, the energy associated with surface tension is minimized by the sidewall grain boundaries “zipping up,” placing the film under tension. It is not clear how this mechanism would extend to oxide films that grow inward at the metal–oxide interface. The mechanism of growth stress for $\alpha\text{-Al}_2\text{O}_3$ scale may be similar. In the case of the scale, growth stress likely continues long past island coalescence, so the mechanism may be generalized to a rough interface minimizing surface energy by a similar zipping process. Growth stress falls to zero either as the interface becomes smoother, or as the average stress in the films is reduced by the film becoming thicker.

A microscopic study of the scales has shown that films exhibiting a large transient tensile growth stress grow with a columnar morphology through their entire thickness, while those with lower growth stress grow with an initially more equiaxed morphology (Tortorelli *et al.*, 2003). This equiaxed morphology may promote a smoother growth surface, minimizing the stress produced by surface tension and the “island coalescence” mechanism. Evans and Cannon (1989) point out that columnar oxides experience larger growth stress because displacements at grain boundaries normal to the interface do not contribute to stress.

Another mechanism for a tensile growth stress is proposed by Cannon and Hou (1998). If Al and O vacancies are at equilibrium at the scale surface and the scale–metal interface, vacancies will be supersaturated at cracks and voids in the scale, recombining at these sites and leading to high tensile stress in thin scales. In thicker scales, creep by the substrate will relieve stress in the scale.

CONCLUSIONS

High-temperature alloys based on FeCrAl and NiAl are heated in air at temperatures ranging from 1000 °C to 1200 °C. Techniques have been developed for X-ray stress analysis of the resulting $\alpha\text{-Al}_2\text{O}_3$ scale in times as short as 5 min. Transient tensile stresses are observed, with magnitudes

ranging from zero in Kanthal to ~ 1 GPa in NiAl, NiAlHf, and FeCrAlY. The stress persists for times > 12 h at 1000° and ~ 0.5 h at 1200°. Because applied thermal stress relaxes much more quickly, observed growth stresses must reflect a dynamic equilibrium between stress generation and relaxation.

The observed tensile stresses are inconsistent with the Pilling–Bedford mechanism, which predicts compressive stress in all cases. One alternative is the conversion of transitional Al_2O_3 to $\alpha\text{-Al}_2\text{O}_3$, for which the Pilling–Bedford mechanism does predict tensile stress. Transitional Al_2O_3 is observed for one alloy (NiAl) only, during the growth period where tensile stress is observed. A more widely applicable alternative mechanism is the “zipping up” of the grain boundaries at a rough interface, where surface tension provides the energy to put the film under tensile stress.

ACKNOWLEDGMENTS

Research sponsored by the Division of Materials Sciences and Engineering, U.S. Department of Energy (DOE), under Contract No. DE-AC05-00OR22725 with UT-Battelle, LLC. The UNICAT facility at the Advanced Photon Source (APS) is supported by the University of Illinois at Urbana—Champaign, Materials Research Laboratory (U.S. DOE, the State of Illinois-IBHE-HECA, and the National Science Foundation), ORNL, the National Institute of Standards and Technology (U.S. Department of Commerce) and UOP LLC. The APS is supported by the U.S. DOE, Basic Energy Sciences, Office of Science under Contract No. W-31-109-ENC-38.

- Bull, S. J. (1998). *Oxid. Met.* **49**, 1–17.
 Busing, W. R. and Levy, H. A. (1966). *Acta Crystallogr.* **22**, 457.
 Cannon, R. M. and Hou, P. Y. (1998). In *High-Temperature Corrosion and Materials Chemistry*, edited by P. Y. Hou, M. J. McNallan, R. Oltra, and D. A. Shores (The Electrochemical Society, Pennington, NJ).
 Evans, A. G. and Cannon, R. M. (1989). *Mater. Sci. Forum* **43**, 243–268.
 Evans, H. E. (1989). *Mater. Sci. Eng. A* **120**, 139–146.
 Evans, H. E. (1994). *Mater. High Temp.* **12**, 219–227.
 Floro, J. A., Hearne, S. J., Hunter, J. A., Kotula, P., Chason, E., Seel, S. C., and Thompson, C. V. (2001). *J. Appl. Phys.* **89**, 4886–4897.
 Goto, T., Anderson, O. L., Ohno, I., and Yamamoto, S. (1989). *J. Geophys. Res.* **94**, 7588–7602.
 Grabke, H. J. (1999). *Intermetallics* **7**, 1153–1158.
 Huntz, A. M. (1988). *Meas. Sci. Technol.* **4**, 1079–1088.
Kanthal Appliance Heating Alloys Handbook, The Kanthal Corporation, Bethel, CT.
 Levin, I. and Brandon, D. (1998). *J. Am. Ceram. Soc.* **81**, 1995–2012.
 Messaoudi, K., Huntz, A. M., and Di Menza, L. (2000). *Oxid. Met.* **53**, 49–75.
 Nix, W. D. and Clemens, B. M. (1999). *J. Mater. Res.* **14**, 3467–3473.
 Noyan, I. C. and Cohen, J. B. (1987). *Residual Stress* (Springer-Verlag, New York).
 Pilling, N. B. and Bedworth, R. E. (1923). *J. Inst. Met.* **29**, 529–582.
 Sarioglu, C., Blachere, J. R., Pettit, F. S., and Meier, G. H. (1997). In *Microscopy of Oxidation 3*, edited by S. B. Newcomb and J. A. Little (The Institute of Materials, London), pp. 41–51.
 Sarioglu, C., Schumann, E., Blachere, J. R., Pettit, F. S., and Meier, G. H. (2000). *Mater. High Temp.* **17**, 109–115.
 Schumann, E., Sarioglu, C., Blachere, J. R., Pettit, F. S., and Meier, G. H. (2000). *Oxid. Met.* **53**, 259–272.
 Schütze, M. (1997). *Protective Oxide Scales and their Breakdown* (Wiley, Chichester).
 Stott, F. H. and Atkinson, A. (1994). *Mater. High Temp.* **12**, 195–207.
 Tortorelli, P. F., More, K. L., Specht, E. D., and Zschack, P. (2003). *Mater. High Temp.* **20**, 303–310.
 Veal, B. W. (personal communication).